ELSEVIER

Biophysical Chemistry 115 (2005) 295–302

Biophysical Chemistry

http://www.elsevier.com/locate/biophyschem

Protein stability and ligand binding: new paradigms from in-silico experiments

Chandra S. Verma[a,*], Stefan Fischer[b]

[a]*Bioinformatics Institute, 30 Biopolis Way, #07-01 Matrix, Singapore-138671, Singapore*
[b]*Computational Molecular Biophysics, Universität Heidelberg, IWR, Im Neuenheimer Feld 368, room 203, D-69120 Heidelberg, Germany*

Received 19 July 2004; received in revised form 26 November 2004; accepted 10 December 2004
Available online 5 January 2005

Abstract

Computer simulations are used to investigate two features of proteins: ligand binding and ligand entry/exit. Both reveal surprising new insights into the physics of such complex systems and suggest at possible interpretations that depart from the usual paradigms. A ligand binding study using normal mode analysis suggests that, contrary to the perceived notion that ligand binding induces a tightening of the protein (as would be evidenced by a blue shift in its vibrational spectrum), there seem to be cases where ligand binding causes an increase in the entropy through a red-shift in the vibrational spectrum of the protein; this occurs in the part of the spectrum that is associated with large-scale low-frequency delocalized motions of proteins. Moreover, this increase seems to be dependent on the ability of the ligand to form hydrogen bonds within the polar cavity of the protein. This suggests an additional driving force for stabilizing complex formation. In parallel, pathways of ligand access to cavities in two proteins are mapped and it is found that, in agreement with recent interpretations of experimental data emerging from NMR studies, these pathways are characterized by a ruggedness of the energy landscape, which leads to a picture that has a physically more appealing basis than the traditional two-state paradigm normally invoked for ligand binding.

Keywords: Computer simulations; Ligand binding; Ligand entry; Entropy; Ruggedness

1. Introduction

Computer simulations have come of age, in that they are now regularly able to complement experimental data on fundamental processes that underlie biology [1,2] and have been a major complement to modern structural biology [3]. This has partly come about from advances in hardware, software and theory on the one hand and partly from experimental advances on the other; the latter have served to explore spatial and temporal regimes that are accessible to computer calculations. The traditional strength of simulations in providing rich and detailed models at a static level [3–6] is now regularly complemented by reports of increasingly predictive power at a dynamic level [7].

Given the confidence that this approach now elicits, it is appropriate and timely that the technique may be extended to explore avenues that have traditionally been considered well established. There are two particular areas that we examine here. First, we examine the structural and energetic changes that accompany ligand binding. Traditionally, the paradigm of structural biology holds that a protein tightens when a ligand binds to it. Upon examination of a set of complexed and uncomplexed structures, we see that indeed this is apparently true as judged by a reduction in the interatomic spacing. There are forces such as hydrogen bonds and hydrophobic forces that stabilize a ligand and hold it in a binding cavity. The binding and approach of atoms to each other results in electronic redistributions around, for example, two polar atoms (oxygen and nitrogen), which leads them to attract each other. So if a ligand were to form say three hydrogen bonds with the protein cavity atoms, then the distance between the protein cavity

* Corresponding author. Tel.: +65 64788273; fax: +65 64789047.
E-mail address: chandra@bii.a-star.edu.sg (C.S. Verma).

0301-4622/$ - see front matter © 2004 Elsevier B.V. All rights reserved.
doi:10.1016/j.bpc.2004.12.038

atoms will be somewhat smaller in the complexed situation, relative to the uncomplexed. While this makes sense on the one hand, on the other, we must remember that it is only a localized phenomena. A protein is a dynamic entity with a hierarchy of motions occurring on multiple time and length scales [8–10], each linked to functionality in a manner that has not yet been characterized comprehensively; nevertheless, progress is being made [11,12]. So we examine this issue from a global perspective of the changes taking place in the whole protein–ligand complex. The other issue that we set out to examine is one of the pathway of ligand (un)binding. This itself is made up of two parts: are there characteristic pathways of ligand binding [13]; is the traditional two-state paradigm [14], which has so successfully explained (and continues to explain) biochemical processes and phenomena always sufficient [15]?

2. Methods

We use water as a ligand in our studies and examine its binding to the protein bovine pancreatic trypsin inhibitor (BPTI). In particular, we focus on one buried water molecule that makes four near-optimal hydrogen bonds and has been observed in the same binding pocket repeatedly using both crystallography and NMR [16]. The representations and descriptions of the interatomic interactions of the system have been described before [16] and have been shown to be adequate in reproducing experimental data [16,17]. Briefly, to examine the changes that occur in BPTI upon ligand binding, extensive energy minimizations were carried out on BPTI; this was followed by normal mode analyses of BPTI with and without the bound water [18–20]. The advantage of using normal mode analytical methods is that they can be used to decompose motions into a set of orthogonal vectors, which can then be manipulated in detail to find out exactly what, how and where changes in the vibrational spectra and hence the associated vibrational entropies take place [20]. As the observations have been described in greater detail elsewhere [20], we only refer to the essential results here; we additionally report previously uncharacterized results whereby the effects of deuterated water (D_2O) and the role of electrostatics have been examined (Part A of the Results section).

To examine ligand entry pathways, we charted the energetics of the paths that water takes to enter a polar cavity in BPTI (the same cavity considered above) and additionally, those that benzene takes to enter a hydrophobic cavity that was created in a mutant Lysozyme, Leu99Ala; this latter has been characterized experimentally [21]. In order to represent bulk solvent as a continuum, we have used a new method of scaling the charges [22]. The pathways were computed using reaction path methods that have been shown to reproduce experimental data on activated processes quite reasonably well [16,17]. Detailed analyses of these pathways are being presented elsewhere [Fischer and Verma, in preparation] and we only summarize the findings here (Section 3.1).

3. Results

3.1. Part A

The computed enthalpic change for a water molecule binding to a polar cavity in the protein BPTI [18] is ~−21 kcal mol^{-1} (~−20 kcal mol^{-1} for D_2O binding to the same cavity). This is unsurprising since the binding is driven by the formation of four near-optimal hydrogen bonds. The concomitant structural changes in the protein are minimal (~0.1 Å over backbone atoms including a decrease in the inter-atomic separation across the active site of up to ~0.8 Å as the formation of hydrogen bonds with the buried water brings the polar atoms in the cavity closer together). The polar interactions result in a strong electrostatic interaction (~−16 kcal mol^{-1}) between the water and the protein (the interaction of D_2O is marginally weaker at −15 kcal mol^{-1}), which is partly offset by weakened intra-protein interactions (~+3.5 kcal mol^{-1}). This latter is an indication of a global weakening of the protein and was reflected in the computed vibrational entropic changes that occur on this complexation; we find that the computed entropy content of the BPTI–water complex is ~13.4 cal mol^{-1} K^{-1} larger than that of uncomplexed BPTI (stabilizing the overall free energy change by 4 kcal mol^{-1} at 300 K); in contrast, upon D_2O binding, the entropy increase is somewhat larger, at 15.1 cal mol^{-1} K^{-1} (stabilizing the overall free energy change by 4.5 kcal mol^{-1}). A dissection of the entropic changes as a function of the vibrational spectrum (Fig. 1) shows that this increase of 13.4 cal mol^{-1} K^{-1} in H_2O and of 15.1 kcal mol^{-1}in D_2O arises from changes largely below 1000 cm^{-1}. This change can be decomposed into two parts: a 4 cal mol^{-1} K^{-1}increase as circled in Fig. 1 and the rest of the increase of 9.4 cal mol^{-1} K^{-1} (or 11.1 cal mol^{-1} $K^{-1}$for D_2O). The larger increase arises from a transformation of the translational–rotational–vibrational modes of the 9 degrees of freedom of a water molecule (or D_2O), that is free to rotate/translate in bulk water, to restricted translations–rotations–vibrations within the protein cavity. While these modes are mixed with the modes of the protein [20], to get an idea of the actual frequencies, we carried out normal mode analyses of H_2O/D_2O in the fixed protein and these and their corresponding entropic contributions are shown in Fig. 1 and in Table 1. Of course, the higher frequency modes, corresponding to the O–H (or O–D) stretching and H–O–H (or D–O–D) angle bending modes undergo a small blue shift (which is expected upon the formation of hydrogen bonds between the water and the atoms of the protein cavity); anyway their contribution to the entropic change is negligible. It is clear that the difference between H_2O and D_2O arises from the larger mass of the latter, resulting in its librational modes being somewhat red-shifted

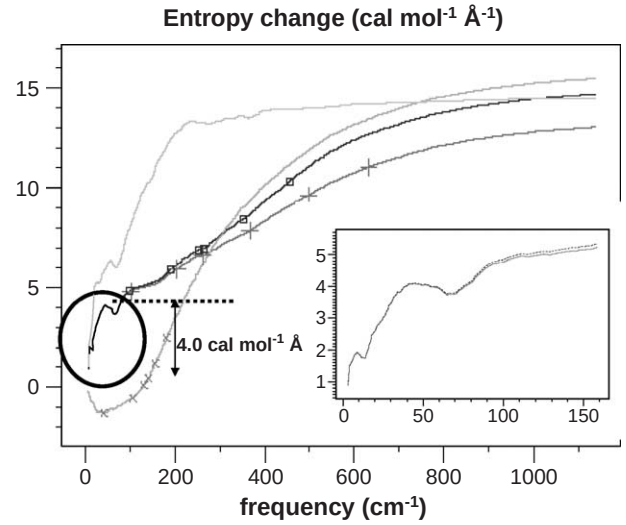

Fig. 1. The cumulative change in the vibrational entropy (in cal mol^{-1} K^{-1} along the-axis) upon binding of H_2O (red), D_2O (in blue); uncharged-H_2O (in green) to a polar cavity in BPTI and the difference between the H_2O-bound and the Gly36Ser mutant (in yellow). Data for frequencies up to 1300 cm^{-1} only are shown as the curves stabilize by 1200 cm^{-1}. The symbols represent the frequencies of libration of H_2O, D_2O or uncharged-H_2O in the protein cages and are given in Table 1. The circled region shows the 4 cal mol^{-1} K^{-1} increase in entropy associated with the low frequency region of the spectrum and further highlights the fact that it is separate from the point at which the librational frequencies of the buried water appear. (Inset) A zoomed view of the spectrum below 150 cm^{-1} is shown to highlight the similarity in increase in both H_2O (solid red line) and D_2O (dotted blue line). (For interpretation of the references to colour in this figure legend, the reader is referred to the web version of this article.)

relative to that of H_2O (and hence the larger entropic content). Among the librational modes, the contributions from the three lowest frequency modes is the same for both systems; the major difference (1.4 cal mol^{-1} K^{-1}) arises from the next three modes.

The remainder 4 cal mol^{-1} K^{-1} increase in the overall entropic change arises from a loosening of the protein; the hump in the initial part of Fig. 1 (inset) shows that this loosening arises from the low-frequency part of the vibrational spectrum; this is the region that is associated with the slow, large amplitude motions of proteins (often the functional modes). What is interesting is that, in the case of both H_2O and D_2O, this increase is the same (Fig. 1, inset).

So we decided to examine if the electrostatic interaction between the protein and bound water played any role. For this, the computations were repeated but with the charges on the water atoms set to 0.0. This again resulted in an enthalpic stabilization upon water (with point charges on the oxygen and the two hydrogens set to 0.0) binding; however, there is a significant drop to −4.9 kcal mol^{-1} which is unsurprisingly made up largely by van der Waals interactions (−4.5 kcal mol^{-1}). The corresponding van der Waals interactions for H_2O and D_2O were similar (−4.1 and −3.2 kcal mol^{-1}, respectively). What is more interesting is that now the lower frequency part of the spectrum is merged with the librational modes of the "uncharged" water (in contrast to a clear separation in the case above) and there is a destabilization of the entropic change in the low frequency region (see green curve in Fig. 1, inset). This suggests that the local tightening around the polar cavity caused as a result of electrostatic interactions between H_2O/D_2O and the polar protein atoms leads to a global loosening of the protein; however, this does not seem to happen if this local interaction is replaced by a more apolar interaction, as evidenced by the switching off of the point charges on the water atoms. As a further test, we examined the mutant Gly36Ser, which has been studied experimentally and is known to be somewhat less stable than the wild type [23]. The introduced serine residue is known to replace the buried water with its sidechain hydroxyl group and the four hydrogen bonds that water makes are now replaced with only three hydrogen bonds. In our computations, the root mean squared difference between the Gly36Ser mutant and

Table 1
Vibrational modes and corresponding entropies of water (H_2O, D_2O and uncharged-water) obtained by computing the modes vibration of H_2O and D_2O in the fixed protein, BPTI

Mode no.	H_2O		D_2O		Uncharged-H_2O	
	Frequency (cm^{-1})	Entropy (cal mol^{-1} K^{-1})	Frequency (cm^{-1})	Entropy (cal mol^{-1} K^{-1})	Frequency (cm^{-1})	Entropy (cal mol^{-1} K^{-1})
1	102	3.4	100	3.5	43	5.1
2	204	2.1	191	2.2	106	3.4
3	261	1.7	252	1.7	132	2.9
4	366	1.1	263	1.6	142	2.8
5	497	0.7	352	1.2	157	2.6
6	631	0.4	455	0.8	183	2.3
7	1776 (1737)	$4*10^{-3}$	1295 (1265)	$3*10^{-2}$	1743 (1737)	$5*10^{-3}$
8	3357 (3323)	$3*10^{-6}$	2437 (2406)	$2*10^{-4}$	3325 (3323)	$4*10^{-6}$
9	3434 (3370)	$2*10^{-6}$	2502 (2469)	$3*10^{-4}$	3373 (3370)	$3*10^{-6}$
	Total	9.4		11.1		19.1

For the fixed protein analysis, the mass-weighted Hessian matrix is computed for the complex and is then reduced to diagonalization of the 9×9 block matrix that is made up of elements H_{ij} where i and j are coordinate indices of the atoms of the water molecule. Values in parentheses are the vibrational frequencies of H_2O/D_2O/uncharged-H_2O alone.

the wild type is only 0.6 Å over all nonhydrogen atoms with changes localized to the loop region that surrounds the cavity. The overall vibrational entropy is ~15 cal mol^{-1} K^{-1} lower than the wild type; however, the interesting feature is that the loss of a hydrogen bond in the cavity leads to a decrease in the vibrational entropy of ~6 cal mol^{-1} K^{-1} in the same region of the spectrum (below 100 cm^{-1}) as was seen in the case of H_2O. Of course, the two situations are somewhat different in that, whereas H_2O is bound non-covalently to the protein, Ser is attached covalently leading no doubt to other contributory differences. Nevertheless, it strengthens the argument that hydrogen bonds in the polar cavity of BPTI are important in modulation of the global dynamics of the protein. We hypothesize that these hydrogen bonds result in the formation of anchor points, which can act as pivots for enhanced global fluctuations. A more comprehensive and detailed analysis of the dynamics of a further series of mutants of BPTI is currently being addressed (Somani and Verma, in preparation). Indeed, entropic stabilization of the free energy (i.e., an increase in entropy) upon complexation in different systems has been reported by others [24,25].

We find that, while the localization of the water in the binding pocket and the subsequent formation of the four near-optimal hydrogen bonds leads to a local tightening of the complex, the overall vibrational spectrum of the complex undergoes a red-shift, i.e., it becomes loose. Further, the resulting increase in flexibility occurs in that part of the spectrum, which is not only decoupled from the changes that take place as a result of the water molecule's librational modes, but take place predominantly in modes of motion that represent large-scale collective motions, delocalized over the whole structure of the protein (for motions that are characterized by frequencies lower than 50–100 cm^{-1}). A similar change was seen when the number of hydrogen bonds formed in the cavity is modulated by the design of a mutant (Gly36Ser). A recent study that explored the free energy of binding of the water to BPTI is in agreement with our findings [25]. The role of disorder and perhaps incumbent promiscuity is a relatively unexplored avenue and has been linked to biochemical processes such as signalling, DNA-binding, metal-induced activation [26–29], etc. Our work and that of others [24] suggest that buried waters might play a significant role in modulating the flexibility (disorder) and hence the functionality of proteins. We hope that this study will stimulate further work in this field.

Having explored some aspects of the thermodynamics that governs ligand binding, using the binding of water to a polar cavity in the protein BPTI as a paradigm, we now turn our attention to the pathways that this water molecule takes to enter this binding site; this binding site is occluded from the bulk and hence atomic fluctuations will open transient pathways through which the water can enter/exit. We examine the energetics that underlie the kinetics of this process.

3.2. Part B

The diffusion of ligands into and out of, and within the protein matrix, has been a subject that has long been investigated both experimentally and theoretically, most notably using the protein myoglobin as a testbed [30,31]. The question that has not yet been answered unambiguously is: are there distinct pathways to buried cavities in proteins that are accessible to ligands?

One of the key findings that was reported some years ago was the discovery of alternate ligand binding pathways in myoglobin [13] in contrast to the classical view that ligand entry routes were limited to those that accessed the bulk from regions very close to the porphyrin moiety which is the site for ligand binding. Indeed, this view of limited numbers of pathways for ligand binding still largely dominates thinking, although combinations of experiments and theory suggest departures from this [32]. This is further coupled to the largely appealing and simple two-state paradigm governing the events associated with ligand binding (and protein folding): ligand bound↔ligand unbound; protein folded↔protein unfolded (see for example Ref. [33]); this view has traditionally been invoked to model binding data quite successfully.

In an important study, Denisov et al. [15] developed novel techniques of NMR to examine the binding of water to BPTI in some detail and concluded that the standard two-state paradigm needed some revision. When their data was fitted using the standard Arrhenius paradigm, they found that the enthalpic barriers required for the process of ligand entry are ~22 kcal mol^{-1}. But this process occurs on a timescale that is similar to that on which activated processes such as Phe rings flip in the packed interior of proteins; however, these processes have activation barriers that are far lower, of the order of 10–15 kcal mol^{-1} (see for example Ref. [17]). So how do we reconcile this apparent conflict? The answer seems to lie in looking at this process using a formalism that is different from the traditional two-state paradigm. Halle and colleagues report that their data could as well be fitted using the empirical Ferry's law; this latter has been used successfully by solid state physicists to model ligand diffusion in matrices. The essential difference between the two-state Arrhenius paradigm and that proposed by Ferry is that whereas the former is a functional of the form $A\ \exp(\Delta H^{\#}/RT)$, the latter is characterized by $A\ \exp[\Delta H^{\#}/RT+\langle H_1^2\rangle/(RT)^2]$. Fig. 2 summarizes the two behaviours with the continuous line representing the Arrhenius two-state scenario and the jagged line representing the Ferry formalism. The two figures are based on the equivalence of reproduction of experimental data by Halle and coworkers using either of the two formalisms [15].

We have investigated the process of entry of ligands into proteins by computing several pathways of entry of water into the polar cavity of BPTI (the same cavity that is mentioned in Section 3.1) and of benzene into a cavity that was created by mutating a buried Leu to Ala (at position 99)

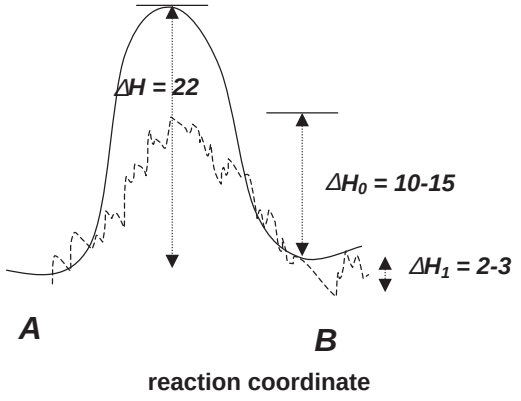

Fig. 2. The energy profiles (y-axis) along the reaction coordinates (x-axis, arbitrary units) for ligand binding (state A represents the unbound state and state B represents the bound state). The smooth continuous curve represents the two-state Arrhenius formalism; the broken curve represents Ferry's law. The symbols represent the energy barriers as in the text. The values are energy barriers in kcal mol^{-1}. Figure is based in analogy with that shown in [15].

in T4 Lysozyme [34]. While a detailed and comprehensive analysis is being presented elsewhere (Fischer and Verma, in preparation) and has been partly communicated earlier [35], we present here the essential findings that are common to the various pathways that the ligands take to access the cavities buried within proteins.

The pathways are characterized by multiple minima separated by multiple transition states (Figs. 3a and 5a) with barriers of the order of 10–15 kcal mol^{-1}. The process of entry of water into BPTI is characterized by a complex conformational energy landscape where protein–water interactions and protein deformations are dominant and these dynamics translate into ruggedness of the order of 1–2 kcal mol^{-1}. The underlying physical basis of this ruggedness is the change in energetics during the formation, breakage and reformation of noncovalent interactions (hydrogen bonds and/or van der Waals interactions) as the protein fluctuates and accommodates the entering ligand (see http://www.bii.a-star.edu.sg/~chandra/Biophyschem-BIFI.ppt) [15,33]. As is evident from Fig. 3b, these changes are of the order of 1–3kT; this also is the magnitude of energetics that underlie room temperature fluctuations of proteins [30,33]. The highest barrier to entry shown here for the BPTI–water system is 13.6 kcal mol^{-1} for the path shown here. These barriers are similar to those that characterize other microsecond processes in proteins on timescales similar to the water entry timescales [16,17]). The major components to the barrier are the interaction between protein and water as the water enters through a transient opening in the region where the sidechain of Tyr35 is packed against the backbone of the Arg39–Ala40 region (see Fig. 4a,b), aided by a hydrogen bond to the hydroxyl of Tyr35. The barrier of 13.6 kcal mol^{-1} is made up of ~8 kcal mol^{-1} destabilization of the protein–water electrostatic interactions while the protein deformations contribute ~5 kcal mol^{-1}. A similar (4–6 kcal mol^{-1}) energetic strain arises from deformation of the protein *dihydrofolate reductase* as it accommodates the rotation of a buried Phe ring [36]. In another study, we found that protein–water interactions of this very same water (as in this study) are destabilized by ~8.8 kcal mol^{-1} to accommodate its C_2-flip within the polar cavity [37]; the protein–water interactions in the current study of water entry are destabilized similarly (by 8.2 kcal mol^{-1}).

In order to examine the role of electrostatics of the ligand in the entry process, we repeated the calculations with uncharged-water entering BPTI. Again, the profiles of the

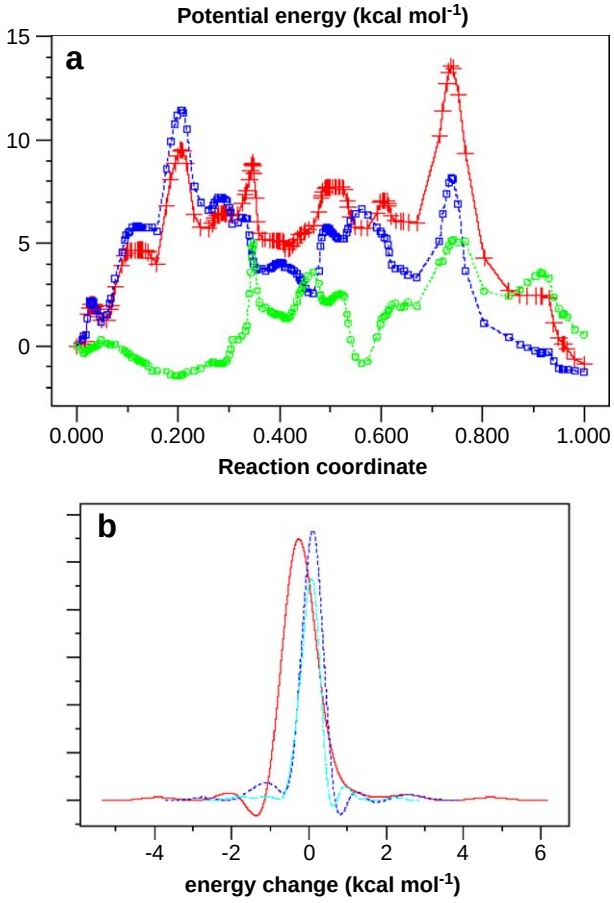

Fig. 3. (a) The energetic profiles characterizing the pathways of entry of water into BPTI computed using reaction path methods as outlined [16,17]. The highest peak (13.6 kcal mol^{-1}) corresponds to the barrier mentioned in the text. In red is the total potential energy relative to the reference state, which is the state with the protein and the water unbound, while its two main components, i.e., the protein–water interactions and the protein deformation energies, are shown in dashed blue and green lines, respectively. The y-axis is the energy (in kcal mol^{-1}) along the reaction coordinate (x-axis; the reaction path is the sum up to a given point of the path of the root mean square difference in coordinates between successive pairs of intermediate structures along the path and is normalized here so that a value of 0 represent the state when the ligand is outside the protein and a value of 1 is the state when the ligand is in its bound state within the protein). (b) The distribution of energy changes (difference between subsequent conformations) along the pathway of water entering BPTI: red is total energy change; blue is BPTI–water interaction energy change; cyan is protein (deformation) energy change; the y-axis is the probability distribution in arbitrary units. (For interpretation of the references to colour in this figure legend, the reader is referred to the web version of this article.)

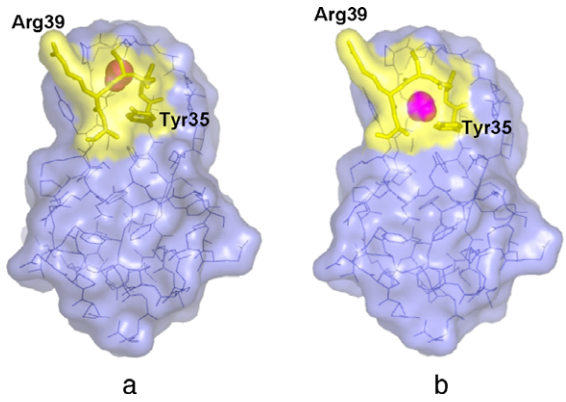

Fig. 4. The structure of wild type BPTI with (a) the water bound to the polar cavity and (b) the transition state of the water entry (this is the state with the highest potential energy along the computed pathway). The water molecule is shown as magenta spheres. The region Tyr35–Ala40 is shown highlighted in yellow; this is the region through which the water enters the protein matrix. (For interpretation of the references to colour in this figure legend, the reader is referred to the web version of this article.)

energetics of the pathway are similar to that for charged-water–BPTI or for benzene–Lysozyme with a similar ruggedness (Fig. 5a,b). This latter is unsurprising because they originate in the dynamic (re)formation of non-covalent interactions which will be similar irrespective of whether the ligand is charged or not. In the case of the uncharged-water, the barrier, which originates with the water entering the protein from the same region as seen for charged-water (Fig. 4), reduces significantly (by ~5.5 kcal mol^{-1}) to ~8.2 kcal mol^{-1} (Fig. 5a) and is dominated by protein deformations; as anticipated, the van der Waals interactions between the uncharged-water and the protein contribute only about *kT*. A similar pattern is seen for uncharged, hydrophobic benzene entering the mutant Lysozyme (Fig. 5b) where the barrier to entry is similar, at ~9 kcal mol^{-1} and is dominated by protein deformations (not shown). In BPTI, the water-binding cavity is fairly close to the surface and so it is easy to imagine that the entry of the ligand does not require large fluctuations in the protein. However, the cavity in Lysozyme is deep inside the protein and sterically inaccessible, judging by graphical visualizations of the crystal structure. And yet, the fluctuations required to accommodate the ligand are ~1 Å in BPTI and somewhat larger (~2–3 Å) in Lysozyme. Graphical inspections show that the reason they do not require large movements and therefore high energies is because they are the result of several small-scale motions that typically characterize the room temperature fluctuations of the atoms that make up the protein matrix. These motions dynamically open up transient cavities that are occupied by the ligand [38]. Of course, the occupation of a cavity by a ligand itself perhaps induces the opening of additional cavities [39]. This nonlinear progression of sequential openings of cavities is also brought about from the coupling of the motions of large regions of the protein (see http://www.bii.a-star.edu.sg/~chandra/Biophyschem-BIFI.ppt). Together, they give rise to energetic profiles that are rugged as discussed above. While the reduction of barriers due to the large scale motions is hard to quantify in the present study, nevertheless, they must play an important role and it must be that evolutionary constraints and the nature of the amino acid sequences must be very important.

The binding pathways of both ligands show a remarkable similarity in the profiles of the overall energetics that characterize the binding, despite the fact that there is a two-fold difference in the size of the ligands. Additionally, the energetics of the deformations of the proteins along the

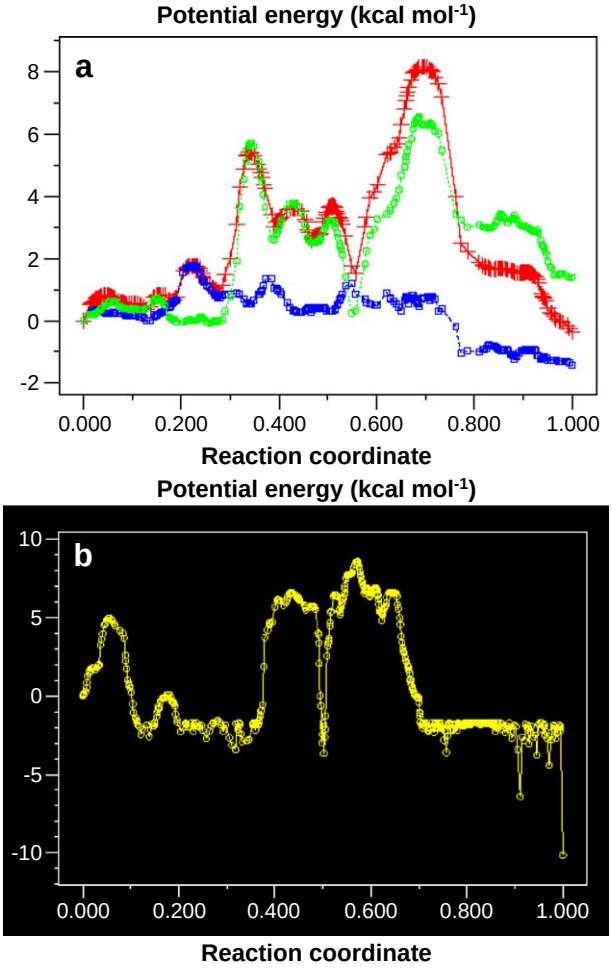

Fig. 5. (a) The energetic profiles characterizing the pathways of entry of uncharged-water into BPTI computed using reaction path methods as outlined [16,17]. The highest peak (8.2 kcal mol^{-1}) corresponds to the barrier mentioned in the text. In red is the total potential energy relative to the reference state, which is the state with the protein and the water unbound, while its two main components, i.e., the protein–water interactions and the protein deformation energies, are shown in dashed blue and green lines, respectively. The *y*-axis is the energy (in kcal mol^{-1}) along the reaction coordinate (as described in legend to Fig. 3). (b) The energetic profile characterizing the pathways of entry of benzene into the Leu99Ala mutant T4 Lysozyme computed using reaction path methods as outlined in [16,17]. The highest peak (~9 kcal mol^{-1}) corresponds to the barriers that are mentioned in the text. The *y*-axis is the total potential energy (in kcal mol^{-1}), relative to the reference state which is the state with the protein and benzene unbound, along the reaction coordinate (as described in legend to Fig. 3). (For interpretation of the references to colour in this figure legend, the reader is referred to the web version of this article.)

pathways are similar to those that are seen in other activated processes in proteins (with similar timescales). Electrostatic interactions between the protein and the ligand (water) increase the barrier to entry. Moreover, our computations seem to suggest that, at least in the class of reactions involving the diffusion of small molecules into proteins, the Ferry's formalism, as invoked by Halle and colleagues, whereby ligand entry is limited by barriers ($\Delta H^{\#}$) of the order of 10–15 kcal mol^{-1} and a ruggedness (H_1) of 1–2 kcal mol^{-1}, certainly seems to provide a model with an intuitive physical basis. We are currently extending this study to other systems.

4. Conclusion

We find that there are situations whereby ligand binding can entropically stabilize a protein, particularly through enhancing global delocalized motions through the formation of hydrogen bonds; this suggests an additional force that drives ligand binding and will be important in computational efforts to design ligands for proteins. The entry (and hence exit) of such ligands into proteins is characterized by pathways that require relatively similar and small fluctuations (distortions) of the proteins and are aided by motions that couple the whole protein together. Ligands that are nonpolar seem to diffuse with barriers that are lower than those for polar ligands. Computational calculations suggest an intuitively appealing picture of the energy landscapes that govern protein–ligand interactions, in line with experimental observations.

Acknowledgements

This work was carried out while one of us (CSV) was at the York Structural Biology ab, Dept. of Chemistry, Univ. of York, York YO10 5HZ, UK prior to joining BII. BII is an A-STAR institute. Structural images were drawn with Pymol (W.L. DeLano "The Pymol Molecular Graphics System", DeLano Scientific LLC, San Carlos, CA, USA. http://www.pymol.org") and graphics were created using SQUID [40].

References

[1] M. Karplus, J.A. McCammon, Molecular dynamics simulations of biomolecules, Nat. Struct. Biol. 9 (2002) 646–652.
[2] B.L. de Groot, H. Grubmuller, Water permeation across biological membranes: mechanism dynamics of aquaporin-1 and GlpF, Science 294 (2001) 2353–2357.
[3] M.K. Gilson, T.P. Straatsma, J.A. McCammon, D.R. Ripoll, C.H. Faerman, P.H. Axelsen, I. Silman, J.L. Sussman, Open "back door" in a molecular dynamics simulation of acetylcholinesterase, Science 263 (1994) 1276–1278.
[4] R.A. Bockmann, H. Grubmuller, Nanoseconds molecular dynamics simulation of primary mechanical energy transfer steps in F1-ATP synthase, Nat. Struct. Biol. 9 (2002) 198–202.
[5] M. Karplus, Y.Q. Gao, Biomolecular motors: the F1-ATPase paradigm, Curr. Opin. Struck. Biol. 14 (2004) 250–259.
[6] M.A. Young, S. Gonfloni, G. Superti-Furga, B. Roux, J. Kuriyan, Dynamic coupling between the SH2 and SH3 domains of c-Src and Hck underlies their inactivation by C-terminal tyrosine phosphorylation, Cell 105 (2001) 115–126.
[7] W.L. Jorgensen, The many roles of computation in drug discovery, Science 303 (2004) 1813–1818.
[8] M. Akke, J.J. Liu, J. Cavanagh, H.P. Erickson, A.G. Palmer III, Pervasive conformational fluctuations on microsecond time scales in a fibronectin type III domain, Nat. Struct. Biol. 5 (1998) 55–59.
[9] H. Frauenfelder, S.G. Sligar, P.G. Wolynes, The energy landscapes and motions of proteins, Science 254 (1991) 1598–1603.
[10] I. Bahar, B. Erman, T. Haliloglu, R.L. Jernigan, Efficient characterization of collective motions and interresidue correlations in proteins by low-resolution simulations, Biochemistry 36 (1997) 13512–13523.
[11] H. Frauenfelder, B.H. McMahon, P.W. Fenimore, Myoglobin: the hydrogen atom of biology a paradigm of complexity, Proc. Natl. Acad. Sci. U. S. A. 100 (2003) 8615–8617.
[12] M. Berjanskii, M. Riley, S.R. Van Doren, Hsc70-interacting HPD loop of the j domain of polyomavirus t antigens fluctuates in ps to ns and μs to ms, J. Mol. Biol. 321 (2002) 503–516.
[13] X. Huang, S.G. Boxer, Discovery of new ligand binding pathways in myoglobin by random mutagenesis, Nat. Struct. Biol. 1 (1994) 226–229.
[14] P.A. Jennings, Speeding along the protein folding highway: are we reading the signs correctly, Nat. Struct. Biol. 5 (1998) 846–848.
[15] V.P. Denisov, J. Peters, H.D. Horlein, B. Halle, Using buried water molecules to explore the energy landscape of proteins, Nat. Struct. Biol. 4 (1996) 505–509.
[16] S. Fischer, C.S. Verma, R.E. Hubbard, Rotation of buried water inside a protein: calculation of the rate vibrational entropy of activation, J. Phys. Chem., B 102 (1998) 1797–1805.
[17] C.S. Verma, S. Fischer, L.S.D. Caves, G.C.K. Roberts, R.E. Hubbard, Calculation of the reaction pathway for the aromatic ring flip in methotrexate complexed to dihydrofolate reductase, J. Phys. Chem. 10 (1996) 2510–2518.
[18] S. Fischer, C. Verma, Binding of buried structural water increases the flexibility of proteins, Proc. Natl. Acad. Sci. U. S. A. 96 (1999) 9613–9615.
[19] B. Tidor, M. Karplus, The contribution of vibrational entropy to molecular association. The dimerization of insulin, J. Mol. Biol. 238 (1994) 405–414.
[20] S. Fischer, J. Smith, C. Verma, Dissecting the vibrational entropy change on protein/ligand binding: burial of a water molecule in bovine pancreatic trypsin inhibitor, J. Phys. Chem., B 105 (2001) 8050–8055.
[21] A. Morton, B.W. Matthews, Specificity of ligand binding in a buried nonpolar cavity of T4 lysozyme: linkage of dynamics and structural plasticity, Biochemistry 34 (1995) 8576–8588.
[22] S.M. Schwarzl, D. Huang, J.C. Smith, S. Fischer, How well does charge reparameterization account for solvent screening in molecular mechanics calculations? The example of myosin, In Silico Biol. 3 (2003) 187–196.
[23] K.D. Berndt, J. Beunink, W. Schroder, K. Wuthrich, Designed replacement of an internal hydration water molecule in BPTI: structural and functional implications of a glycine-to-serine mutation, Biochemistry 32 (1993) 4564–4570.
[24] D.K. Phelps, P.J. Rossky, C.B. Post, Influence of an antiviral compound on the temperature dependence of viral protein flexibility packing: a molecular dynamics study, J. Mol. Biol. 276 (1998) 331–337.
[25] L.R. Olano, S.W. Rick, Hydration free energies and entropies of water in protein interiors, J. Am. Chem. Soc. 126 (2004) 7991–8000.
[26] L.M. Iakoucheva, P. Radivojac, C.J. Brown, T.R. O'Connot, J.G. Sikes, Z. Obradovic, A.K. Dunker, The importance of intrinsic

disorder for protein phosphorylation, Nucleic Acids Res. 32 (2004) 1037–1039.
[27] M. Gubler, T.A. Bickle, Increased protein flexibility leads to promiscuous protein–DNA interactions in type IC restriction-modification systems, EMBO J. 10 (1991) 951–957.
[28] J. Villanueva, M. Hoshino, H. Katou, J. Kardos, K. Hasegawa, H. Naiki, Y. Goto, Increase in the conformational flexibility of beta 2-microglobulin upon copper binding: a possible role for copper in dialysis-related amyloidosis, Protein Sci. 13 (2004) 797–809.
[29] M. Madrid, J.A. Lukin, J.D. Madura, J. Ding, E. Arnold, Molecular dynamics of HIV-1 reverse transcriptase indicates increased flexibility upon DNA binding, Proteins: Struct. Funct. Genet. 45 (2001) 176–182.
[30] H. Frauenfelder, B.H. McMahon, P.W. Fenimore, Myoglobin: the hydrogen atom of biology and a paradigm of complexity, Proc. Natl. Acad. Sci. U. S. A. 100 (2003) 8615–8617.
[31] R. Elber, M. Karplus, Enhanced sampling in molecular dynamics: use of the time-dependent hartree approximation for a simulation of carbon monoxide diffusion through myoglobin, J. Am. Chem. Soc. 112 (1990) 9161–9175.
[32] R.C. Wade, P.J. Winn, I. Schlichting, Sudarko, A survey of active site access channels in cytochromes P450, J. Inorg. Biochem. 98 (7) (2004 (Jul)) 1175–1182.
[33] J.N. Onuchic, P.G. Wolynes, Theory of protein folding, Curr. Opin. Struck. Biol. 14 (2004) 70–75.
[34] V.A. Feher, E.P. Baldwin, F.W. Dahlquist, Access of ligands to cavities within the core of a protein is rapid, Nat. Struct. Biol. 3 (1996) 516–521.
[35] D.G. Truhlar, W.L. Jorgensen, M.T. Nguyen, J.B. Anderson, D. Chandler, S. HammesSchiffer, P.G. Bolhuis, I.H. Hillier, C. Dellago, J.N.L. Connor, M.V. Basilevsky, J.C. Tully, J.M. Bowman, E.M. Goldfield, G. Katz, T.J. Martinez, W. Jakubetz, H.W. Schranz, K.J. Schulten, M. Sprik, G.C. Schatz, J.T. Hynes, I.H. Williams, P.R. Taylor, C.S. Verma, A. Lagana, K. Morokuma, C. Trindle, H.F. Schaefer, N.A. Burton, L. Blancafort, Faraday Discuss. 110 (1999) 477–520.
[36] C.S. Verma, S. Fischer, L.S.D. Caves, G.C.K. Roberts, R.E. Hubbard, Calculation of the reaction pathway for the aromatic ring flip in methotrexate complexed to dihydrofolate reductase, J. Phys. Chem. 100 (1996) 2510–2518.
[37] S. Fischer, C.S. Verma, R.E. Hubbard, Rotation of structural water inside a protein: calculation of the rate and vibrational entropy of activation, J. Phys. Chem., B 102 (1998) 1797–1805.
[38] H.-X. Zhou, S.T. Wlodek, J.A. McCammon, Conformational gating as a mechanism for enzyme specificity, Proc. Natl. Acad. Sci. U. S. A. 95 (1998) 9280–9283.
[39] S.K. Ludemann, V. Lounnas, R.C. Wade, How do substrates enter and products exit the buried active site of cytochrome P450cam?1. Random expulsion molecular dynamics investigation of ligand access channels and mechanisms, J. Mol. Biol. 303 (2000) 797–811.
[40] T.J. Oldfield, SQUID: a program for the analysis and display of data from crystallography and molecular dynamics, J. Mol. Graph. 10 (1992) 247–252.